Eur. Phys. J. D **37**, 181–186 (2006)
DOI: 10.1140/epjd/e2005-00283-5

THE EUROPEAN PHYSICAL JOURNAL D

Experimental oscillator strengths of Zn II lines of astrophysical interest

R. Mayo, M. Ortiz[a], and J. Campos

Facultad de Ciencias Físicas, Dpto. de Física Atómica, Molecular y Nuclear, Universidad Complutense de Madrid, 28040 Madrid, Spain

Received 6 April 2005 / Received in final form 18 July 2005
Published online 25 October 2005 –

Abstract. Relative transition probabilities for 18 lines of Zn II (11 measured for the first time) were determined from the emission-line intensities in a laser-produced plasma. The experiment was carried out using Cd–Zn alloy with a Zn content under 10% in order to obtain optically thin plasma. Oscillator strengths were placed on an absolute scale by using experimental lifetimes, line-strength sum rules and Boltzmann plot. A comparison has been conducted between present experimental results, the data available and new calculations reported in this work, as well as a study of the plasma conditions.

PACS. 52.70.Kz Optical (ultraviolet, visible, infrared) measurements – 32.70.Cs Oscillator strengths, lifetimes, transition moments – 32.70.Fw Absolute and relative intensities

1 Introduction

There has been continuous interest in the determination of $4p\ ^2P_{1/2}$ and $4p\ ^2P_{3/2}$ resonant level lifetime of single ionised zinc. After the pioneering work of Baumann and Smith [1] who used the phase-shift method, radiative lifetimes measurements have been made with beam-foil [2–4], zero-field [5] and laser induced fluorescence in a hollow cathode lamp [6]. Apart from that, after the works of Andersen et al. [5] and Bergeson and Lawler [6], some experimental oscillator strengths have been reported in the NIST tables [7].

Theoretical calculations for these lifetimes have been performed using on different methods: Coulomb approximation [4,8], Hartree-Fock [9,10], Dirac-Fock [11] and one-electron model approach [12,13].

Because of the great advancement in astrophysics due to the Goddard High Resolution Spectrograph on the Hubble Space Telescope, atomic data for many ions are of increasing interest [14–16]. Zinc has been identified in Be stars [17] and experimental data for absorption lines from the ground level [18] are also available. From cosmology to stellar atmospheres dynamics, Zn II plays an important role in many research fields within astronomy and astrophysics [19–22]. That is why, accurate abundances measurements of this ion are important [23,24]. This fact has renewed the interest in Zn II oscillator strength determination and new resonant levels measurements [25,26] and calculations have been published recently. For other excited levels nevertheless, both measurements and calculations are scarce.

Thus, the aim of this work is to provide new experimental and calculated values of oscillator strengths and verify the previously existing. To our knowledge, for 11 of these there are no experimental values available in the literature.

The relative oscillator strength for the Zn II studied lines have been measured by determining the emission line intensity of laser produced plasmas of Zn–Cd alloys with a low zinc content. Self-absorption of the Zn II transitions has been studied, taking into account plasma temperature, electron density and upper levels population. The best conditions to carry out the measurements were created using 1–10% Zn–Cd alloys. In order to place the data on an absolute scale, experimental lifetimes (where available) [26], line-strength sum rules and the Boltzmann plot were applied.

In order to identify the transitions the compilation article of Sugar and Musgrove [27] and the paper of Gullberg [28] have been used. Theoretical vales were obtained in Intermediate Coupling (IC) by the least square fitting (LSF) method with multiconfigurational interaction and using ab initio Hartree-Fock calculations made with Cowan's computer code [29]. To provide level energies for our calculations, the aforementioned reference of Sugar and Musgrove [27] has been used.

2 The experiment

A Q-switch Nd-YAG laser generates 200 mJ pulses of 7 ns at 20 Hz frequency and 10 640 Å wavelength. The laser beam was focused onto the target with a 12.5 cm focal

[a] e-mail: campos@fis.ucm.es

length lens. The sample was placed into a chamber filled with argon at 8 Torr. In order to obtain good statistics, it was necessary to provide unexposed material for consecutive laser pulses, so the target was mounted on a rotating shaft. In order to ensure a clean environment, the chamber was evacuated to 0.2 Torr and was being refilled with argon while the inside pressure was increasing.

The light emitted from the plasma region was registered by a 1 m Czerny-Turner spectrometer at right angles with respect to the laser beam. A time-resolved optical multichannel analyzer (OMA III, EG&G) allowed the detection at present times of spectrum sections of the laser pulse, during a selected time length. An automatically background accumulation and subtraction for every spectrum was made. The data were stored in a computer for further analysis. The resolution of the spectroscopic system to separate two close lines was 0.30 Å in first order and the spectral range was from 1900 to 7000 Å.

The measurements were carried out for delay times of 100, 200, 300 and 500 ns (Fig. 1) with respect to the laser shot and the light was collected for 50 ns. Each spectrum was averaged of 50 laser shots signals. Measured branching fractions did not depend on the delay time but the best signal-to-noise ratio was observed at 300 ns delay time. Therefore, the data analysis was performed at this delay time.

The spectral efficiency of the system was measured obtaining the spectra of calibrated deuterium (1900–3300 Å) and quartz-tungsten (2850–7000 Å) lamps with 450 Å overlapping region. The final calibration was the result of the overlapping joint regions of these two lamps employing a least-square fitting procedure. The calibration of the system was also checked by measurements of the branching ratio of well-known Ar I and Ar II spectral lines. The two types of calibration were in agreement within an error limit of 5%. In order to check the photodiode sensitivity, the 431.6 nm KrI spectral line was registered on different channels of the detector (50 channel steps in a 1024 array). The maximum sensitivity difference of photodiode groups was 2%. The final error due to the efficiency calibration was estimated to be around 6%.

For the spectral analysis, special care has been taken to identify the Zn II lines. In the plasma can be found lines due of ions with several degrees of ionisation. To detect line spectral blending in the Zn–Cd spectra, plasma measurements on pure Cd and Zn samples were carried out. NIST [7] wavelength tables and the temporal evolution intensity of the lines have also been taken into account.

Numerically, the spectral analysis was made by fitting the line profiles to a generated Voigt profile, which is the convolution of Lorentzian profile from Stark broadening with Gaussian profile from Doppler and instrumental broadening. The line intensity corresponds to the area under the line profile and the final experimental result for each line was the average of six different measurements. The final instrumental profile of the registration system was obtained through analysis of narrow lines of hollow cathode lamps.

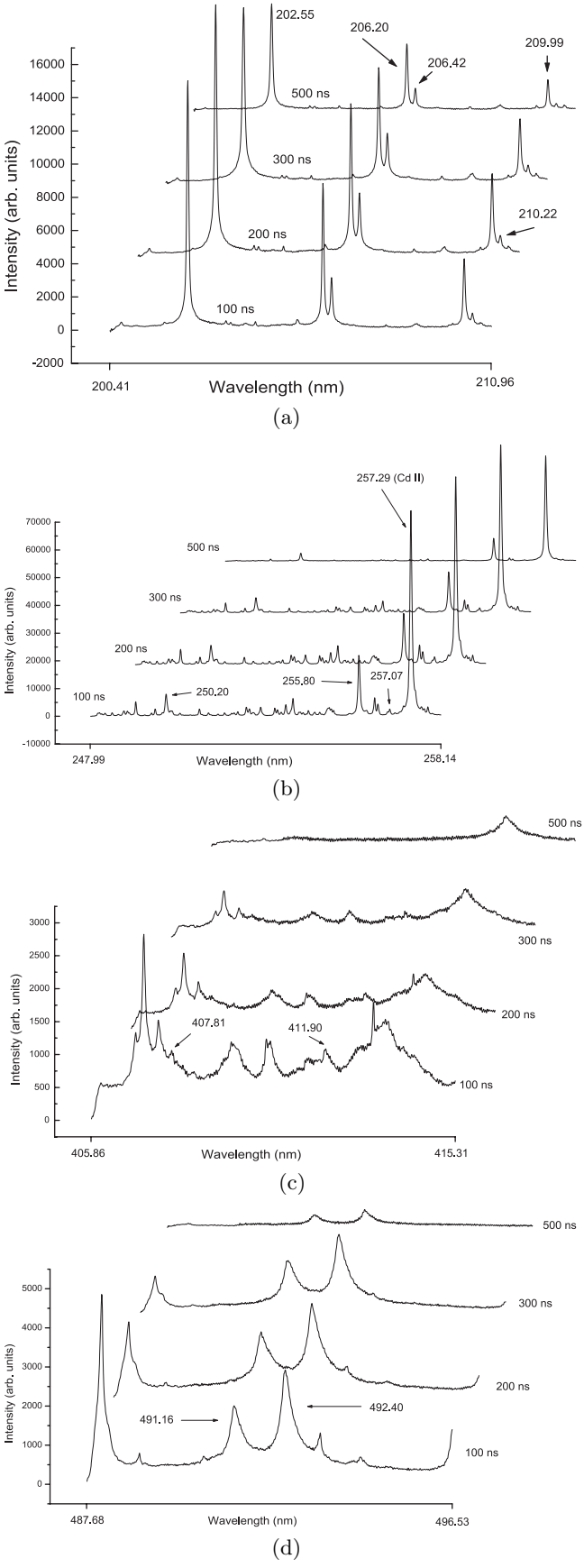

Fig. 1. Temporal evolution of Cd–Zn spectrum.

Table 1. Temporal evolution of some Cd–Zn plasma parameters.

Delay Time (ns)	T (K)	N_e (10^{16} cm^{-3})	Composition		
			N(ZnII)/N(ZnI)	N(CdII)/N(CdI)	N(CdII)/N(ZnII)
100	12 700 ± 1800	17.64 ± 1.41	16.94	16.35	59.65
200	13 500 ± 2100	17.10 ± 1.37	29.58	28.44	53.14
300	13 600 ± 2100	16.56 ± 1.32	23.08	31.21	74.01
500	11 400 ± 1400	16.43 ± 1.31	6.52	6.34	161.42

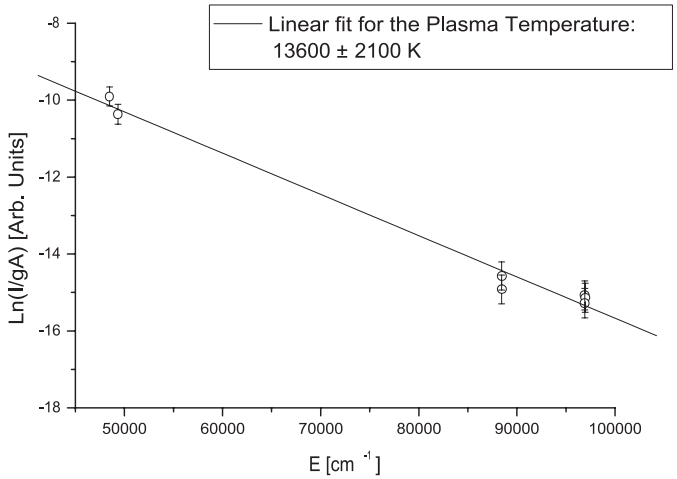

Fig. 2. Boltzmann plot of the plasma temperature.

As aforementioned, we used Cd–Zn alloys with zinc content under 10%. The reason for this is to avoid self-absorption effects in the present experiments. No dependence of the branching ratios on concentration has been observed in the 5–1% range of zinc content.

3 Plasma diagnostics

Plasma electron density, estimation of the upper levels population, temperature and self-absorption of the Zn II transitions were studied in order to find the best experimental conditions for carrying out the measurements. In order to estimate the mentioned self-absorption, in these experimental conditions with the calculation of the absorption coefficient of the most intense lines of Zn II in our spectral range, we must prove existence of the Local Thermodynamic Equilibrium (LTE).

The temperature for the Cd–Zn alloy in our experimental conditions was 13 600 ± 2100 K. This value was derived from a Boltzmann plot for Zn II obtained with the line intensities and the transition probabilities of the present experiment. This Boltzmann plot (Fig. 2) was made with the oscillator strengths values obtained for the transitions from $5s\ ^2\mathrm{S}_{1/2}$ and $4d\ ^2\mathrm{D}_{3/2}$ with the use of experimental branching ratios and the oscillator strengths results derived from the LIF experiment of Blagoev et al. [26] for the radiative lifetimes of the resonant lines from $4p$ and the line from $4d\ ^2\mathrm{D}_{5/2}$ due to the fact from these three upper levels only one line decays and, consequently, the inverse of the radiative lifetime is the transition probability, i.e. the oscillator strengths.

The electron density in our experimental conditions was derived from the Stark broadening of the 2062.00 Å line of Zn II. The theoretical data of Popović et al. [21] were employed and a value of $N_e = (1.66 \pm 0.13) \times 10^{17}$ cm^{-3} was obtained. The error comes from the statistical uncertainties of the measured line widths. The Thorne criterion [30] for the electron density under the assumption of LTE is given by:

$$N_e(\mathrm{cm}^{-3}) \gg 1.6 \times 10^{12} \sqrt{T(\mathrm{K})}\,[\Delta E(\mathrm{eV})]^3 \qquad (1)$$

where N_e is electron density, T is plasma temperature and ΔE is the highest energy difference between the upper and lower states for all transitions studied. For this work, the highest difference is 6.4 eV, therefore by applying this value to the Thorne criterion and using the calculated temperature, we obtained an upper limit of $N_e \geq 4.9 \times 10^{16}\,\mathrm{cm}^{-3}$. Due to the fact that the electron density in our experiment was $N_e = 1.66 \times 10^{17}$ cm^{-3} it could be concluded that the plasma was in LTE during the monitored time interval.

After obtaining the temperature and the electron density, Saha's equation was applied and the plasma compositions for the ionic species were obtained. For this calculation we evaluated the contribution of the different ions with a partition sum up to $4s5d\ ^3\mathrm{D}_3$ for ZnI, $4f\ ^2\mathrm{F}_{5/2}$ for ZnII, $5s5d\ ^3\mathrm{D}_3$ for CdI and $5d\ ^2\mathrm{D}_{5/2}$ for CdII. The final plasma compositions were $N(\mathrm{ZnII})/N(\mathrm{ZnI}) = 23.08$, $N(\mathrm{CdII})/N(\mathrm{CdI}) = 31.21$ and $N(\mathrm{CdII})/N(\mathrm{ZnII}) = 74.01$. Both temperature and electron density values as well as these results for plasma composition were determined for a 300 ns delay time from the laser shot.

In Table 1 the different temperature, electronic density and ionic species compositions are shown as an example of the temporal evolution of the plasma conditions. Besides, with a spline fit for all the parameters except for the electronic density where an exponential decay fit was used, in Figures 3 and 4 we plot these tables, that is, the evolution of the plasma conditions with the time after the laser shot.

An estimation of the plasma self-absorption can be calculated using the electron density obtained. The total density of Zn II can be deduced from the corresponding electron density and the ratio of the concentration of different stage ions present in the plasma. Therefore, we have to integrate the line intensity absorption along the line profile for each line in our experiment (where the Lorentzian part in the Voigt profile is predominant due

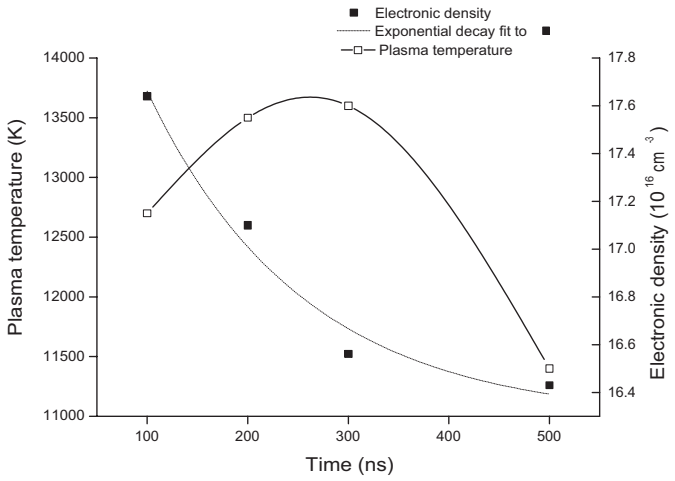

Fig. 3. Temporal evolution of the electronic density and the plasma temperature.

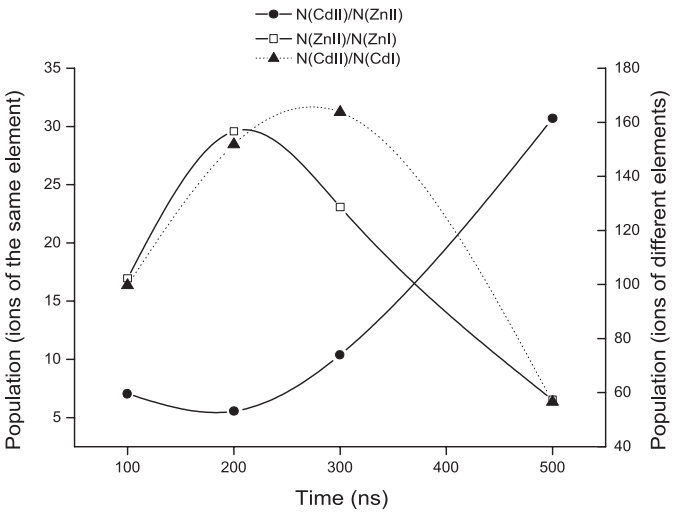

Fig. 4. Temporal evolution of some density ratios among the plasma components.

to the Stark broadening produced by the strong electric fields into the plasma). In fact, we calculate the ratio between the observed intensity and the one emitted by an optically thin plasma, whose condition is [30]

$$K(\lambda)D[\text{cm}] \ll 1. \tag{2}$$

If this ratio exceeds 0.98, what it would be equivalent to a self-absorption lower than 2%, the plasma can be considered to be as optically thin. Due to the highest self-absorption coefficient $K(\lambda)$ was 3.5×10^{-3} cm^{-1} for the line 2062.00 Å of Zn II and that for a plasma thickness of 1 mm the criterion (2) was extensively fulfilled, we can consider that the experiment was carried out in optically thin plasma.

4 Oscillator strengths measurements

The transitions studied are in the range 1900–6200 Å and correspond to lines arising from the $4p$, $4d$, $4f$, $5s$, $5p$, $5d$ and $7s$ electron configurations of Zn II (all of them with a ^{1}S core). Their relative intensity values were obtained from measurements of line-emission intensities of a laser-produced plasma, which was optically thin for the studied lines.

In order to put on absolute scale the relative oscillator strength values two methods were used depending on the data available for radiative lifetime and on the existence of more than one line arising from an upper level. Thus, by measured branching ratios for the case of upper states $5s\ ^2\mathrm{S}_{1/2}$ and $4d\ ^2\mathrm{D}_{3/2}$ and the use of the experimental lifetimes reported by Blagoev et al. [26] the oscillator strengths of those four transitions from those levels could be obtained on an absolute scale.

The rest of transition probabilities presented in this work (that is the lines from the upper levels $4p\ ^2\mathrm{P}_{1/2,3/2}$, $4d\ ^2\mathrm{D}_{5/2}$, $4f\ ^2\mathrm{F}_{5/2,7/2}$, $5p\ ^2\mathrm{P}_{1/2,3/2}$, $5d\ ^2\mathrm{D}_{3/2,5/2}$ and $7s\ ^2\mathrm{S}_{1/2}$) were placed on an absolute scale by using a Boltzmann plot of temperature. After obtaining the plasma temperature from the Boltzmann plot, the transition probabilities for the rest of the lines can be deduced comparing their relative intensities with those of other lines of known transition probabilities taking into account that the LTE condition is satisfied. The transition probability ratio is obtained with the formula [14]

$$I_1/I_2 = (A_1 g_1 \lambda_2 / A_2 g_2 \lambda_1) \exp(\Delta E_{21}/kT) \tag{3}$$

where I denotes the relative intensity measured, λ he transition wavelength, A the transition probability of the spontaneous emission, ΔE the difference of the excitation energy, g the corresponding statistical weight, T is the electron temperature of the plasma in LTE and k is the Boltzmann constant. After obtaining the transition probabilities, they were introduced as oscillator strength values though the expression [30]

$$g_{low} f = 1.499 \times 10^{-8} \lambda^2 g_{up} A \tag{4}$$

where f is the oscillator strength, λ is the transition wavelength in Å, A is the transition probability in 10^8 s^{-1} and g is the corresponding statistical weight for the lower and the upper level of the transition.

The experimental errors associated to the oscillator strength values have been calculated taking into account the statistical uncertainties (ranging around 8%, depending on each line), the experimental errors of the spectral response determination (6%) and the errors associated to the measured radiative lifetimes. For those cases where the temperature was used for obtaining the oscillator strength, the error derived from its determination was also added (15%). The total error is about 20% for most of the studied transitions, except for the lines in which the branching fractions could be used, whose error is about 13%.

5 Results and discussion

Tables 2 and 3 show oscillator strengths for lines arising from the levels of Zn II $4p$, $4d$, $4f$, $5s$, $5p$, $5d$ and $7s$ studied

Table 2. Experimental results for Zn II oscillator strengths.

			f exp								
Upper	Lower	λ(Å)	T.W.	[26]	[6]	[3]	[1]	[2]	[4]	[5]	[7]
$4p\ ^2P_{1/2}$	$4s\ ^2S_{1/2}$	2062.00	0.249 (50)	0.249(29)	0.256(26)		0.209(18)		0.306(58)		0.246
$4p\ ^2P_{3/2}$	$4s\ ^2S_{1/2}$	2025.48	0.467 (93)	0.480(55)	0.488(49)	0.513(60)	0.606(53)	0.62(6)	0.590(84)	0.406(41)	0.501
$4d\ ^2D_{3/2}$	$4p\ ^2P_{1/2}$	2064.23	0.543 (70)								0.588
	$4p\ ^2P_{3/2}$	2102.17	0.087 (11)								
$4d\ ^2D_{5/2}$	$4p\ ^2P_{3/2}$	2099.94	0.69 (14)	0.684(57)		0.704(75)	0.258(47)				0.555
$4f\ ^2F_{5/2}$	$3d^9\ 4s^2\ ^2D_{3/2}$	1929.03	0.00227 (45)								
	$4d\ ^2D_{3/2}$	4911.63	0.99 (20)								0.868
$4f\ ^2F_{7/2}$	$4d\ ^2D_{5/2}$	4924.01	1.32 (26)								
$5s\ ^2S_{1/2}$	$4p\ ^2P_{1/2}$	2501.99	0.185 (24)				0.244(44)	0.16			
	$4p\ ^2P_{3/2}$	2557.95	0.192 (25)				0.128(23)	0.16			
$5p\ ^2P_{1/2}$	$3d^9\ 4s^2\ ^2D_{3/2}$	2782.81	0.00254 (51)								
$5p\ ^2P_{3/2}$	$3d^9\ 4s^2\ ^2D_{3/2}$	2763.92	0.00219 (44)								
	$3d^9\ 4s^2\ ^2D_{5/2}$	2570.65	0.0116 (23)								
$5d\ ^2D_{3/2}$	$5p\ ^2P_{1/2}$	6021.19	0.82 (0.16)								
	$5p\ ^2P_{3/2}$	6111.56	0.0240 (48)								
$5d\ ^2D_{5/2}$	$5p\ ^2P_{3/2}$	6102.49	0.52 (10)								
$7s\ ^2S_{1/2}$	$5p\ ^2P_{1/2}$	4078.13	0.0221 (44)								
	$5p\ ^2P_{3/2}$	4119.39	0.0198 (40)								

0.249 (50) means 0.249 ± 0.050, 0.00227 (45) means 0.00227 ± 0.00045 and so on. T.W. This Work results, [26] LIF (1/Tau), [6] LIF + hollow cathode lamp, [3] Beam-foil (1/Tau), [1] Phase shift (1/Tau), [2] Beam-foil (1/Tau), [4] Beam-foil (1/Tau), [5] Beam Hanle (1/Tau), [7] NIST results.

Table 3. Experimental and theoretical results for Zn II oscillator strengths.

			f exp	f th											
Upper	Lower	λ(Å)	T.W.	T.W.	[26]	[4]	[30]	[11]	[9]	[8]	[32]	[10]	[13]	[33]	[25]	[12]
$4p\ ^2P_{1/2}$	$4s\ ^2S_{1/2}$	2062.00	0.249 (50)	0.317	0.291	0.290	0.260	0.25267	0.238	0.2965	0.2521		0.20	0.2856	0.262	0.268
$4p\ ^2P_{3/2}$	$4s\ ^2S_{1/2}$	2025.48	0.467 (93)	0.642	0.586	0.615	0.515	0.51598	0.487	0.6046	0.5187	0.476	0.41	0.5821	0.537	0.552
$4d\ ^2D_{3/2}$	$4p\ ^2P_{1/2}$	2064.23	0.543 (70)	0.951				0.78489	0.789	0.8477						
	$4p\ ^2P_{3/2}$	2102.17	0.087 (11)	0.0935				0.07952	0.0799	0.08593						
$4d\ ^2D_{5/2}$	$4p\ ^2P_{3/2}$	2099.94	0.69 (14)	0.843	0.757			0.71483	0.718	0.7721		0.67				
$4f\ ^2F_{5/2}$	$3d^9\ 4s^2\ ^2D_{3/2}$	1929.03	0.00227 (45)	0.00316												
	$4d\ ^2D_{3/2}$	4911.63	0.99 (20)	1.08						1.057						
$4f\ ^2F_{7/2}$	$4d\ ^2D_{5/2}$	4924.01	1.32 (26)	1.02						1.009						
$5s\ ^2S_{1/2}$	$4p\ ^2P_{1/2}$	2501.99	0.185 (24)	0.150						0.1274						
	$4p\ ^2P_{3/2}$	2557.95	0.192 (25)	0.147						0.1323		0.113				
$5p\ ^2P_{1/2}$	$3d^9\ 4s^2\ ^2D_{3/2}$	2782.81	0.00254 (51)	0.00191												
$5p\ ^2P_{3/2}$	$3d^9\ 4s^2\ ^2D_{3/2}$	2763.92	0.00219 (44)	0.000331												
	$3d^9\ 4s^2\ ^2D_{5/2}$	2570.65	0.0116 (23)	0.00434												
$5d\ ^2D_{3/2}$	$5p\ ^2P_{1/2}$	6021.19	0.82 (0.16)	0.826						0.9428						
	$5p\ ^2P_{3/2}$	6111.56	0.0240 (48)	0.0787						0.09629						
$5d\ ^2D_{5/2}$	$5p\ ^2P_{3/2}$	6102.49	0.52 (10)	0.708						0.8633						
$7s\ ^2S_{1/2}$	$5p\ ^2P_{1/2}$	4078.13	0.0221 (44)	0.0196						0.0289						
	$5p\ ^2P_{3/2}$	4119.39	0.0198 (40)	0.0188						0.02888						

0.249 (50) means 0.249 ± 0.050, 0.00227 (45) means 0.00227 ± 0.00045 and so on, T.W. This work results, [26] MRHF+core polarisation, [4] Coulomb approximation, [30] relativistic many-body perturbation, [11] MCDF+core polarisation, [9] RHF+core polarisation, [8] Coulomb approximation, [32] Relativistic Supersimmetry Quantum Defect Theory, [10] HF, [13] One-electron approx. with core polarisation, [33] WKB (sinusoidaloscillation), [25] ab initio CI+core polarisation, [12] One electron approximation, model potential.

in this work. These values were obtained from the branching ratio measurements and the experimental lifetime values reported by Blagoev et al. [26] and from a Boltzmann plot of temperature where the first could not be obtained. Besides our results and for the sake of comparison, we also include the previous experimental (Tab. 2) and theoretical results (Tab. 3) from other authors, just mentioning the different methods they used. It has to be pointed out that in Table 2 only Bergeson and Lawler's work [6] shows results for oscillator strengths measured directly; the rest are values derived from radiative lifetime experiments which have been calculated and added in the Table 2.

We made performed theoretical calculations using the MCHFR+IC method, the results of which are also compared in Table 3 with our experimental values. Thus, for the even parity we have used the configurations $4s + 3d^9 4s^2 + 5s + 6s + 7s + 4d + 5d + 3d^9 4s5s + 3d^9 4s4d$ and the $4p + 5p + 6p + 4f + 3d^9 4s4p$ for the odd one, all of them with their corresponding weight and with a least-square fitting for mixed use. The wavefunctions have

been obtained by least-square fitting using experimental energy values [27] and the radial parts of the orbitals with relativistic Hartree–Fock calculation using the code of Cowan [29].

As seen in Table 2, there is a good agreement (30%) between the present experimental values and the previously published ones for different lines. The discrepancies are more significant between experimental and theoretical results (Tab. 3) due to the great number of methods and approximations used throughout the last years. For the present calculations, the discrepancies are within 35% for most of the cases. Besides, important discrepancies in some lines are found. Thus, the transitions from $4d\ ^2\mathrm{D}_{3/2}$ offer different values because these are two oscillator strength values obtained from the measured branching ratios and an experimental radiative lifetime and there is also an important difference between the experimental (1.8 ns, [26]) and the theoretical (1.2 ns) results for the radiative lifetime. Nevertheless, the good reproducibility in the line relative intensities for the branching ratios make us rely on our experimental values. For the lines from $5p\ ^2\mathrm{P}_{3/2}$, the discrepancy can be explained because of its purity, calculated to be around 73% and the cancellation factor associated. This fact can also play an important role in the difference for the line from $5d\ ^2\mathrm{D}_{3/2}$ at 6111.56 Å because it decays to this level.

6 Conclusion

On the basis of accurately obtained spectral lines intensities we have obtained 18 Zn II oscillator strength values, eleven of which measured for the first time. From the available 7 experimental values, only 2 are not derived from radiative lifetime results. A comparison and analysis is also made between the results above, the calculations reported in this work and the calculations available. A study of different plasma conditions with different parameters is also presented.

We would like to thank Prof. Dr. M.C. Sánchez Trujillo and her group of Dpto. Física de los Materiales, Universidad Complutense de Madrid (Spain) for providing the alloys used in this work.

References

1. S.R. Baumann, W.H. Smith, J. Opt. Soc. Am **60**, 345 (1970)
2. T. Andersen, G. Sørensen, J. Quant. Spectrosc. Radiat. Transfer **13**, 369 (1973)
3. I. Martinson et al., Phys. Scripta **19**, 17 (1979)
4. S. Hultberg, L. Liljeby, A. Lindgård, S. Mannervik, E. Veje, Phys. Scripta **22**, 623 (1981)
5. T. Andersen, O. Poulsen, P.S. Ramanujam, J. Quant. Spectrosc. Radiat. Transfer **16**, 521 (1976)
6. S.D. Bergeson, J.E. Lawler, Astrophys. J. **408**, 382 (1993)
7. NIST – Atomic Spectra Data Base Lines (wavelength order) — `http://physics.nist.gov/cgi-bin/AtData/main-asd` (2003)
8. A. Lindgård, L.J. Curtis, I. Martinson, S.E. Nielsen, Phys. Scripta **21**, 47 (1980)
9. J. Migdalek, W.E. Baylis, J. Phys. B **12**, 1113 (1979)
10. O. Zatsarinny, L. Bandurina, J. Phys. B **32**, 4793 (1999)
11. L.J. Curtis, C.E. Theodosiou, Phys. Rev. A **39**, 605 (1989)
12. C. Laughlin, Z. Phys. D **39**, 201 (1997)
13. B.N. Chichkov, V.P. Shevelko, Phys. Scripta **23**, 1055 (1981)
14. S. Djeniže, V. Milosavljević, M.S. Dimitrijević, Eur. Phys. J. D **27**, 209 (2003)
15. E. Biémont, P.H. Lefèbvre, P. Quinet, S. Svanberg, H.L. Xu, Eur. Phys. J. D **27**, 33 (2003)
16. R. Mayo, M. Ortiz, J. Campos, J. Quant. Spectrosc. Radiat. Transfer **94**, 109 (2005)
17. E. Danezis, E. Theodossiou, Astrophys. J. Suppl. Ser. **174**, 49 (1990)
18. D.A. Verner, P.D. Barthel, D. Tytler, Astron. Astrophys. Suppl. Ser. **108**, 287 (1994)
19. M. Pettini, D.L. King, L.J. Smith, R.W. Hunstead, Astrophys. J. **478**, 536 (1997)
20. M. Pettini, L.J. Smith, D.L. King, R.W. Hunstead, Astrophys. J. **486**, 665 (1997)
21. L.Č. Popović, I. Vince, M.S. Dimitrijević, Astron. Astrophys. Suppl. Ser. **102**, 17 (1993)
22. K.C. Smith, Astron. Astrophys. **291**, 521 (1994)
23. B.D. Savage, J.A. Cardelli, U.J. Sofia, Astrophys. J. **401**, 706 (1992)
24. M. Gemišić Adamov, M.M. Kuraica, N. Konjević, Eur. Phys. J. D **28**, 393 (2004)
25. S.A. Harrison, A. Hibbert, Mon. Not. R. Astron. Soc. **340**, 1279 (2003)
26. K.B. Blagoev et al., Phys. Scripta **69**, 433 (2004)
27. J. Sugar, A. Musgrove, J. Phys. Chem. Ref. Data **24** 6, 1803 (1995)
28. D. Gullberg, U. Litzén, Phys. Scripta **61**, 652 (2000)
29. R.D. Cowan, *The Theory of Atomic Structure and Spectra* (Berkeley U. California Press, Los Angeles, 1981)
30. A.P. Thorne, *Spectrophysics* (Chapman and Hall, London, 1988)
31. H.S. Chou, W.R. Johnson, Phys. Rev. A **56** 3, 2424 (1997)
32. S.G. Nana Engo et al., Phys. Rev. A **56** 4, 2624 (1997)
33. G. Lagmago Kamta, S.G. Nana Engo, M.G. Kwato Njock, B. Oumarou, J. Phys. B **31**, 963 (1998)